

Effect of interface recombination on magnetoelectric coupling in CoFe_2O_4 - BaTiO_3 composites

NIE Jun-wu(聂军武), XU Guo-yue(徐国跃), QI Xian-jin(祁先进)

College of Material Science and Technology, Nanjing University of Aeronautics and Astronautics,
Nanjing 211100, China

Received 3 March 2009; accepted 31 March 2009

Abstract: The $(1-x)\text{CoFe}_2\text{O}_4+x\text{BaTiO}_3$ ($x=0.5$) magnetoelectric(ME) nano-powders were prepared by molten salt synthesis method and the corresponding ceramics were sintered. The morphology and structure of as-prepared powders and ceramics were characterized and studied systematically by using XRD, SEM and EDX. In particles, the two phases, CoFe_2O_4 and BaTiO_3 , are symbiotic with nano-scale coordinate lattice. A considerable ME coefficient(α_E) of about 15.96 mV/A is observed in the $x=0.5$ ME ceramic, which is attributed to the better interface sintered by using those nano-particles with the two phases and a correct poling strategy on the sample. But the interface between the phases has gone through a separating and recombining during their sintering process. A two-time sintering process was also performed on those ceramics while the α_E of the $x=0.5$ two-time sintered ceramic drops to 67.7 $\mu\text{V}/\text{A}$, which could be explained by the split of the interface during the recombination in the ceramics preparation.

Key words: magnetoelectric ceramics; molten salt; magnetic properties; interface

1 Introduction

The magnetoelectric(ME) effect is a polarization response to an applied magnetic field H , or a magnetic spin response to an applied electric field E conversely[1]. There is a critical parameter of ME composites to represent the conversion: ME coefficient(α_E), namely, $\alpha_E=\delta E/\delta H$, where δE is the variation of a voltage output response to an applied magnetic field and δH is the change of the magnetic field. A strong ME effect could be achieved from the ‘‘product-property’’ composite consisting of magnetostrictive (MS) and piezoelectric (PE) phases, in which the mechanical deformation due to magnetostriction results in a dielectric polarization due to piezoelectric effects[2]. The requirements of obtaining a high ME effect in ME composites can be summarized by BOOMGAARD et al[3] and LOKARE et al[4] as follows: 1) the two phases in equilibrium and good mechanical coupling between the phases, 2) high piezoelectric and magnetostrictive effect of each phase, and 3) the proper poling strategy in bulk composites.

BOOMGAARD et al[5] firstly synthesized the

composites of cobalt ferrite (CoFe_2O_4 , CFO) with BaTiO_3 (BTO) by the unidirectional solidification of a eutectic composition system Co-Fe-Ba-Ti-O that yielded ME coefficient in 1970s, but α_E was a factor of 40–60 smaller than the calculated theory value. Many researchers[6–8] have taken different fabrication techniques, including directional solidification, sintering and controlled precipitation, to synthesize ME composites in order to obtain higher α_E . It should be noted that the controlled precipitation route provides the ability to synthesize a bulk material with crystallographically aligned nano-scale interfaces and a high interfacial area[9], which in turn controls the microstructure and α_E . The better ferroelectric and ferromagnetic properties in the bulk ME composites, which depend on different synthesis techniques, were extensively emphasized for achieving a high ME effect in the past decade[10–12], but a counterproductive result may arise at the interface between the two phases. In this work, a simple, environmentally friendly synthesis method was used to prepare the CFO-BTO bulk ME composites by molten-salt route, and α_E was measured and compared.

2 Experimental

2.1 Sample preparation

In a typical molten salt synthesis, Co_3O_4 (>99.5%), Fe_3O_4 (>99.3%), BaO (>99.0%), TiO_2 (>99.2%), NaCl and NP-10(nonylphenyl ether) were mixed in a stoichiometric molar ratio of 1:2:3:3:5:3, ground for 20 min, and then sonicated for 10 min. The mixture was transferred to a crucible, pretreated at 400 °C for 2 h, and then loaded into a furnace at 800–820 °C for 20 min, finally cooled to room temperature in air. After washing the quenched material several times with deionized water, the pure CFO-BTO particles were obtained. The powder was pressed into pellets(diameter of 12 mm, thickness of 1.5 mm) and sintered at 1 200 °C for 2 h. After coating those ceramics with silver electrodes on the flat faces, they were electrically polarized in a field of 15–20 kV/cm, kept in 90–130 °C silicon oil for 20 min, then cooled down to room temperature to align the electric dipoles in the piezoelectric phase BTO.

2.2 Characterization

The morphology and structure of nano-particles and ME ceramics were characterized by transmission electron microscope (TEM, FEI–Tecnai20, equipped with EDX), scanning electron microscope (SEM, LEO–1530P, FEI–Quanta200 equipped with EDX) and X-ray diffractometer (XRD, D8 Advance Bruker) with Cu K_α radiation. The piezoelectric coupling coefficient was measured with a d_{33} meter(ZJ–30). Magnetic hysteresis loops for composites were detected using vibrating sample magnetometer(VSM, HH–10) and the ME α_E was measured using lock-in technique[12] employing a dc magnetic field up to 477.5 kA/m and a superimposed ac magnetic signal of less than 796 A/m amplitude at 60 kHz.

3 Result and discussion

In Fig.1, the XRD patterns of the 0.5CFO+0.5BTO nano-composite powders(treated at 800 °C, marked as T1; 820 °C, marked as T2) show that the ferrite spinel structure phase CFO and ferroelectric perovskite structure phase BTO are formed in the powders. The TEM images of the 0.5CFO+0.5BTO nano-composite powders and the EDX spectrum of T2 powder are presented in Fig.2. As seen from Fig.2, the nano-composite powders are synthesized successfully, and the crystallite size of T2 powder is twice that of the T1 powder, which confirms that the temperature is critical to the molten salt method[13]. The elemental analysis using the EDX (Fig.2(c)) shows that the

elements Co, Fe and O are randomly distributed in the piezoelectric BTO matrix, where the Cu peak is related to Cu grid in TEM supporting the sample. According to the XRD results, there is only spinel phase CFO in those powders, which indicates that only the CFO phase is embedded in the BTO matrix in any micro area (300–1 000 nm).

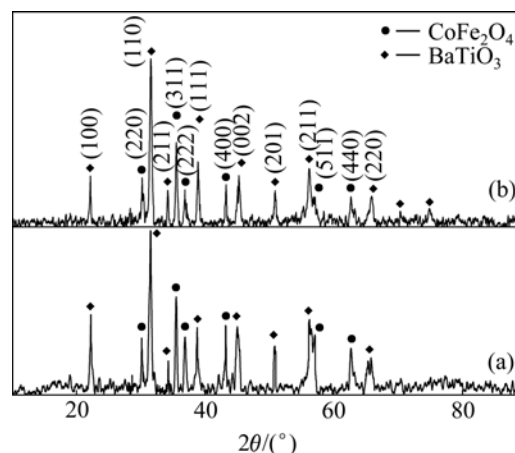


Fig.1 XRD patterns of 0.5CFO+0.5BTO nano-composite powders treated at different temperatures: (a) 800 °C, T1; (b) 820 °C, T2

The lattice parameters of the $(1-x)\text{CFO}+x\text{BTO}$ ME composites ($x=0.5, 0.65$ and 0.8) are calculated by

$$a = d(h^2 + k^2 + l^2)^{1/2} \quad (1)$$

where d is the distance between crystal planes. The values of the parameters are tabulated in Table 1, and the results are in good consistence to the previous studies[10]. On the XRD patterns of the nano-composite powders(Fig.1), the diffraction peak marked the index (110) for the perovskite BTO rightly connects to the peak of index (220) for the spinel CFO. This suggests that the spinel phase is spontaneously separated from the perovskite matrix during growth. There is also an important finding that the ferrite phase lattice parameter is double that of the ferroelectric phases, which is benefit to the construction of a coordinate lattice interface between the two phases. This also presents the possibility that one phase, for example: BTO, could form the octahedron structure on one side of a O^{2-} layer and another phase(CFO) could form the same model but with double size structure on the other side[14]. Because the strain propagates through the interface, the existence of a coordinate lattice interface between the two phases is very important for the production of ME effect, which has also been proved by previous studies[9, 14].

The typical SEM images of the 0.5CFO+0.5BTO ME ceramics sintered with two kinds of pre-powders are shown in Fig.3. The inserts in Fig.3(a) and 3(b) show the micrographs without etching, while the better interface

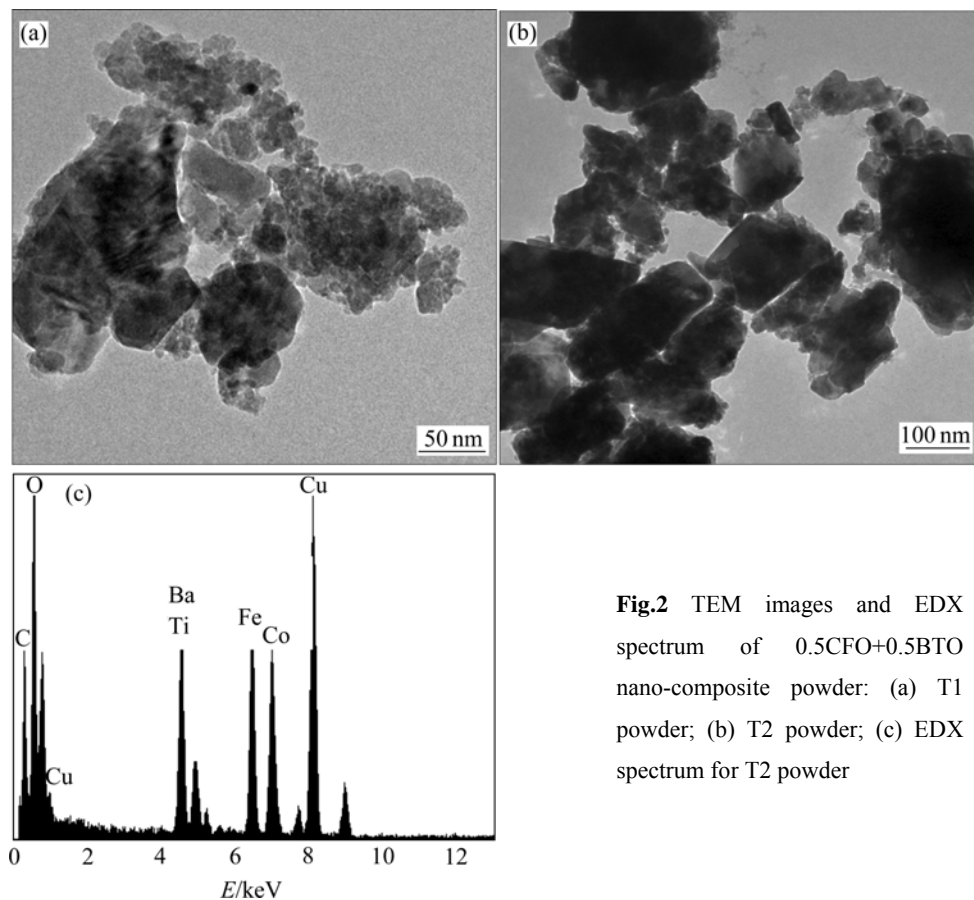


Fig.2 TEM images and EDX spectrum of 0.5CFO+0.5BTO nano-composite powder: (a) T1 powder; (b) T2 powder; (c) EDX spectrum for T2 powder

Table1 Structural, electric and magnetic data of $(1-x)\text{CFO}+x\text{BTO}$ ME ceramics

x	Lattice parameter			Electric resistivity/ ($10^8 \Omega \cdot \text{cm}$) (Poling Temperature)	Poling voltage/ ($\text{kV} \cdot \text{cm}^{-1}$)	$d_{33}/$ ($\text{pC} \cdot \text{N}^{-1}$)	$\alpha_E/$ ($\text{mV} \cdot \text{A}^{-1}$)
	Ferrite phase/ \AA	Ferroelectric phase/ \AA	c/a				
$x=0.5(\text{T1})$	8.39	$a=3.98; c=4.04$	1.01	48(90 $^\circ\text{C}$)	15	9	4.21
$x=0.5(\text{T2})$	8.38	$a=3.97; c=4.02$	1.02	75(90 $^\circ\text{C}$)	18.5	14	15.96
$x=0.65(\text{T2})$	8.38	$a=3.99; c=4.03$	1.01	73(110 $^\circ\text{C}$)	18.5	17	7.94
$x=0.8(\text{T2})$	8.38	$a=3.99; c=4.02$	1.01	76(130 $^\circ\text{C}$)	20	25	0.68

combination is only shown in Fig.3(a). The EDX spectrum (Fig.3(c)) for the white phase shows strong Ba and Ti peaks, with the appearance of weak Co and Fe peaks, which suggests that there is only BTO in this area. On the other hand, the dark phase is identified as CFO since another EDX spectrum (Fig.3(d)) exhibits strong Co and Fe peaks and weak Ba and Ti peaks. Usually, the phase BTO is defined as the matrix in ME composites, that's say, the dark phase can be seen to be uniformly embedded in the matrix in an isolated manner. Moreover, the grain size of the 0.5CFO+0.5BTO T2 ceramic(sintered at 1 200 $^\circ\text{C}$) is controlled in the range of 0.8–1.5 μm , which is in good consistence to the previous studies[4, 8–9] as to obtain the high ME coefficient.

Fig.3(b) shows that the grain size of 0.5CFO+0.5BTO T1 ceramic (sintered at 1 200 $^\circ\text{C}$) is well in the range of 0.5–1 μm , while the connection line of the particles is unconsolidated, which may mean the incompact interface between the grains. Due to the difference of combination between the two phases, the α_E of the 0.5CFO+0.5BTO T1 ceramic is 4.21 mV/A , only one forth that of the T2 ceramic (15.96 mV/A). The higher α_E implies higher elastic coupling between the magnetic and piezoelectric phases, and the lower α_E or the absence of ME effect is most likely due to unfavorable interface conditions although those samples are almost prepared in the same route. The elastic coupling can be transferred by response from the magnetostrictive phase under dc bias to piezoelectric

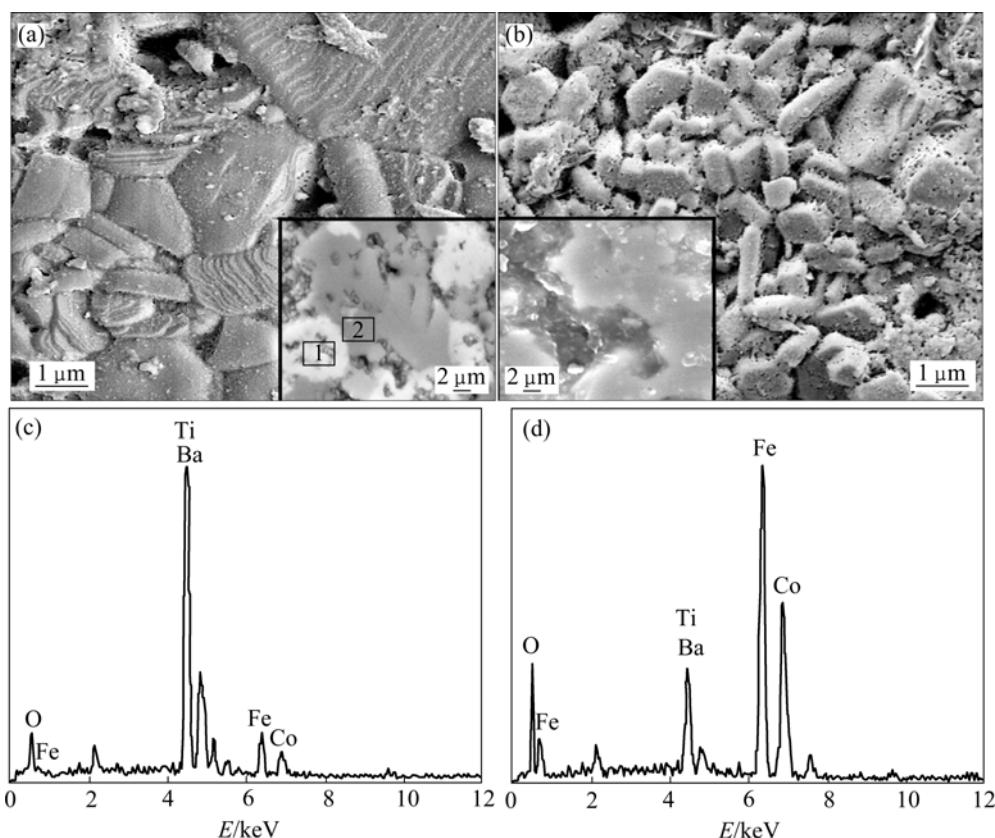


Fig.3 SEM images and EDX spectra of 0.5CFO+0.5BTO ceramics: (a) T2 powder sintered at 1 200 °C (Thermal etching); (b) T1 powder sintered at 1 200 °C (Chemical etching); (c) EDX spectrum from Site 1; (d) EDX spectrum from Site 2

phase. Therefore, having a better interface on the lattice across their grains is important to obtain higher α_E .

In order to strengthen the combination of the interface in the 0.5CFO+0.5BTO ME ceramics, as well as to upgrade their mechanical coupling, the samples were sintered two times at 1 200 °C for 8 h. Figs.4(a) and 4(b) show the SEM images (after thermal etching) of the two-time sintered ME ceramics ($x=0.5$), marked as T12 and T22, respectively. As shown in Fig.4(a), the grain size of T22 keeps within 1–2 μm , while its interface is in better combination compared with that of the T2 sample (see Fig.3(a)). Moreover, the better interface combination with a clear line is also presented in the two-time sintered sample T12 (see Fig.4(b)). Usually, grain growth is at the cost of the same or small grains and is hampered by the grain with different phase finally, which means that recombination of the interface would happen during the two-time sintering process. According to the changes of combination shown in the SEM images, the ME ceramics have better interface after two-time sintering process.

Fig.5 shows the magnetic hysteresis loops of 0.5CFO+0.5BTO powders and the corresponding T1 and T2 ceramics. All ME samples show good magnetic characteristics, indicating the presence of an ordered magnetic structure in both nano-powders and ceramics.

From Fig.5(a), it can be seen that the saturation magnetization(M_s), remnant magnetization(M_r) and coercivity(H_c) of the powders increase a little with treatment temperature rising from 800 °C to 820 °C. The similar results are found in the T2 and T22 ceramic loops, though the two-time sintered ceramic(T22) has gone through a interface recombination. Moreover, the M_s and M_r of T1 ceramic and T12 sample (see Fig.5(c)) are almost consistent, while the H_c has a large increase in T12 ceramic compared with T1 ceramic (from 37.03 kA/m to 51.97 kA/m). This may be attributed to the interface consolidating after the two-time sintering process in the T12 ceramics, as a result, the magnetic domain wall pinning can occur and the H_c increases with the interface consolidation.

Better interface coupling and similar magnetic/dielectric properties are the precondition to obtain high ME coefficient, as expected in the T12 and T22 ceramics. However, a contrary result is obtained, that is, the α_E of T12 ceramic is only 51.8 $\mu\text{V}/\text{A}$, a sharply decrease from 4.21 mV/A of T1 ceramic, which does not meet the anticipative purpose of the properties progress and assumption in this work. Moreover, a similar decrease is presented in the T22 ceramic, that is, the coefficient value $\alpha_E=15.96$ mV/A of T2 ceramic drops to 67.7 $\mu\text{V}/\text{A}$ for T22 ceramic. It is necessary to point out that the

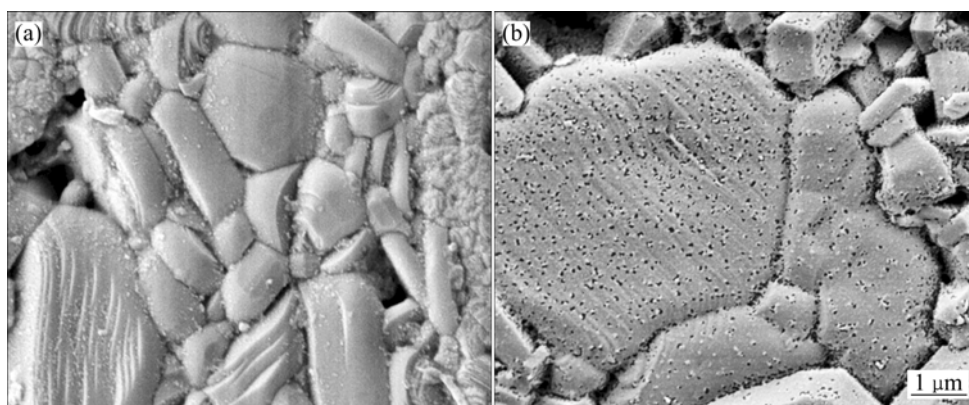


Fig.4 SEM images of 0.5CFO+0.5BTO ceramics: (a) T22 ceramic (two-time sintered at 1 200 °C for 8 h, thermal etching); (b) T12 ceramic (two-time sintered at 1 200 °C for 8 h, thermal etching)

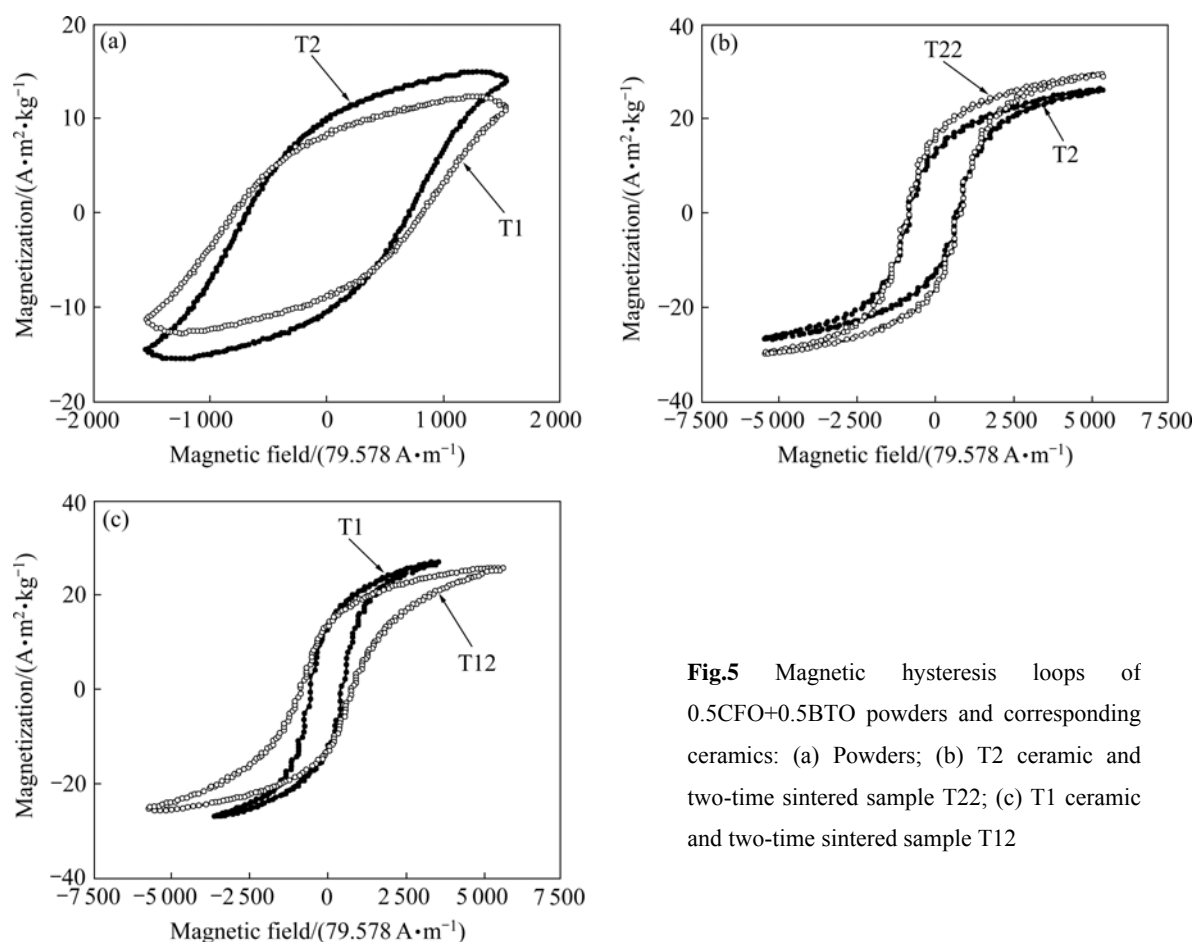


Fig.5 Magnetic hysteresis loops of 0.5CFO+0.5BTO powders and corresponding ceramics: (a) Powders; (b) T2 ceramic and two-time sintered sample T22; (c) T1 ceramic and two-time sintered sample T12

nano-scale coordinate lattice interface between the CFO and BTO phases has to go through recombination during the two-time sintered process and the coordinate lattice split inevitably, while the change of each α_E shows that the interface recombination is not beneficial to α_E after two-time sintering.

The interface coupling factor k [9, 15–18] between the piezoelectric and magnetostrictive phases in the ME composites may represent the change of the interface

recombination. First, set $k=1$ for an ideal interface and 0 for a frictionless case. In the nano-composite powders, there is relatively perfect interface[19] between the phases and the k could be set as 1. After the powders are sintered into ceramics, the interface is combined one time and k drops to less than 0.2 in most of bulk ME composites[16]. According to our studies, the nano-scale coordinate lattice interface between the phases has split completely when the ceramic is sintered two times, but it

does not recover when sintering process is performed on them twice. As a result, the parameter k would decrease to near zero and α_E values go down with it. Several studies[10–12, 19] have proved that nano-particles with coordinate lattice interface in bulk ME composite is beneficial to achieving high ME coefficient. The main reason for deteriorated ME properties in this case needs more study.

4 Conclusions

1) ME nano-composite powders and ceramics were successfully prepared by the molten salt synthesis method and standard sintering method. The XRD, SEM and EDX were used to speculate the interface changes in the powders and ceramics.

2) A maximum value of ME coefficient ($\alpha_E=15.96$ mV/A) is obtained in the case of 0.5CFO+0.5BTO ME ceramic, due to good magnetic/electric characteristics and the proper poling strategy for the ceramic sample.

3) In the two-time sintered ceramics, the ME coefficients of both samples drop to about 75.6 μ V/A, which displays a different result as to our presumption of an increase in α_E . Moreover, the nano-scale coordinate lattice interface between two phases playing a special role in the ME effect is explained.

References

- [1] LANDAU L D, LIFSHITZ E M. Electrodynamics of continuous media [J]. Amer J Phys, 1961, 29(9): 647–648.
- [2] van SUCHTELEN J. Product properties: A new application of composite materials [J]. Philips Res Rep, 1972, 27(1): 28–37.
- [3] van den BOOMGAARD J, van RUN A M J G, van SUCHTELEN J. Piezoelectric-piezomagnetic composites with magnetoelectric effect [J]. Ferroelectrics, 1976, 14: 727–728.
- [4] LOKARE S A, PATIL D R, CHOUGULE B K. Structural, dielectric and magnetoelectric effect in $(x)\text{BaTiO}_3+(1-x)\text{Ni}_{0.93}\text{Co}_{0.02}\text{Mn}_{0.05}\text{Fe}_2\text{O}_4$ ME composites [J]. J Alloy Comp, 2008, 453: 58–63.
- [5] van den BOOMGAARD J, TERRELL D R, BORN R A J. An in situ grown eutectic magnetoelectric composite material [J]. J Mater Sci, 1974, 9: 1705–1708.
- [6] BICHURIN M, PETROV R, KILLIBA Y, BUKASHEV F, SMIRNOV A, ELISEEV D. Magnetoelectric sensor of magnetic field [J]. Ferroelectrics, 2002, 280(1): 199–202.
- [7] COMYN T P, KANGYWE D F, HE J Y, BROWN A P. Synthesis of bismuth ferrite lead titanate nano-powders and ceramics using chemical co-precipitation [J]. J Eur Ceram Soc, 2008, 28: 2233–2238.
- [8] DUONG G, GROESSINGER R. Effect of preparation conditions on magnetoelectric properties of $\text{CoFe}_2\text{O}_4\text{-BaTiO}_3$ magnetoelectric composites [J]. J Magn Magn Mater, 2007, 316: e624–e627.
- [9] PRIYA S, ISLAM R, DONG S, VICHLAND D. Recent advancements in magnetoelectric particulate and laminate composites [J]. J Electroceram, 2007, 19: 147–164.
- [10] MAHAJAN R, PATANKAR K, KOTHALE M, CHAUDHARI S, MATHE V, PATIL S. Magnetoelectric effect in cobalt ferrite-barium titanate composites and their electrical properties [J]. Pramana-J Phys, 2002, 58: 1115–1124.
- [11] SRINIVASAN G, RASMUSSEN E T, BUSH A A, KAMETSEV K E, MESHCHERYAKOV V F, FETISOV Y K. Structural and magnetoelectric properties of $\text{MFe}_2\text{O}_4\text{-PZT}$ ($\text{M}=\text{Ni}, \text{Co}$) and $\text{La}_x(\text{Ca}, \text{Sr})_{1-x}\text{MnO}_3\text{-PZT}$ multilayer composites [J]. Appl Phys A, 2004, 78: 721–728.
- [12] DUONG G, GROESSINGER R, SCHOENHANT M, BUENO-BASQUES D. The lock-in technique for studying magnetoelectric effect [J]. J Magn Magn Mater, 2007, 316: 390–393.
- [13] MAO Y, BANERJEE S, WONG S S. Large-scale synthesis of single-crystalline perovskite nanostructures [J]. J Am Chem Soc, 2003, 125: 15718–15721.
- [14] ECHIGOYA J, HAYASHI S, OBI Y. Directional solidification and interface structure of $\text{BaTiO}_3\text{-CoFe}_2\text{O}_4$ eutectic [J]. J Mater Sci, 2000, 35: 5587–5591.
- [15] FIEBIG M. Revival of the magnetoelectric effect [J]. J Phys D: Appl Phys, 2005, 38: R123–R152.
- [16] SRINIVASAN G, RASMUSSEN E T, HAYES R. Magnetoelectric effects in ferrite-lead zirconate titanate layered composites [J]. Phys Rev B, 2003, 67(014418): 1–10.
- [17] SINGH R S, BHIMASANKARAM T, KUMAR G S, SURYANRAYANA S V. Dielectric and magnetoelectric properties of $\text{Bi}_3\text{FeTi}_3\text{O}_{15}$ [J]. Solid State Commun, 1994, 91: 567–569.
- [18] SRINIVAS A, KIM D W, HONG K S, SURYANARAYANA S V. Study of magnetic and magnetoelectric measurements in bismuth iron titanate ceramic- $\text{Bi}_3\text{Fe}_4\text{Ti}_3\text{O}_{24}$ [J]. Mater Res Bull, 2004, 39: 55–61.
- [19] ZHENG H, WANG J, LOFLAND S E, MA Z, MOHADDES ARDABILI L, ZHAO T, RAMESH R. Multiferroic $\text{BaTiO}_3\text{-CoFe}_2\text{O}_4$ nanostructures [J]. Science, 2004, 30: 661–663.

(Edited by YANG Bing)